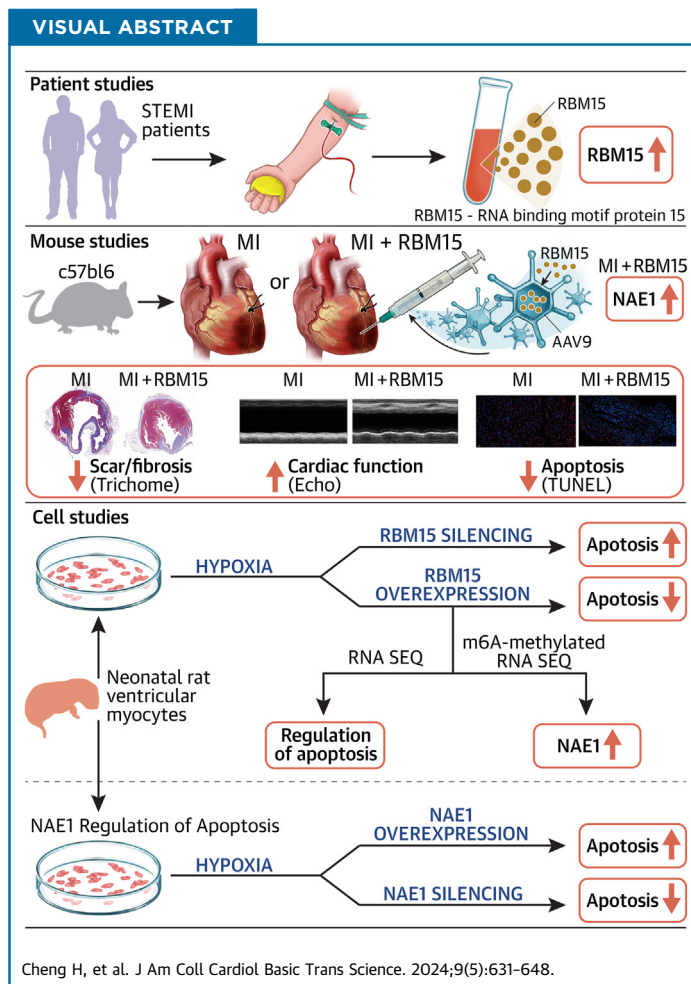


ORIGINAL RESEARCH - PRECLINICAL

RBM15 Protects From Myocardial Infarction by Stabilizing NAE1



Hao Cheng, MD, PhD,^{a,b,c,d,*} Jian Wu, MD, PhD,^{a,b,c,d,*} Linnan Li, MD, PhD,^{a,b,c,d} Xiaoyue Song, MD, PhD,^{a,b,c,d} Junqiang Xue, MD, PhD,^{a,b,c,d} Yuekai Shi, MD, PhD,^{a,b,c,d} Yunzeng Zou, MD, PhD,^{a,b,c,d,e} Jianying Ma, MD, PhD,^{a,b,c,d} Junbo Ge, MD, PhD^{a,b,c,d,e}



HIGHLIGHTS

- RBM15, as a RNA-binding protein, participates in m⁶A regulation in MI.
- RBM15 can attenuate cardiomyocyte apoptosis and improve heart function after MI.
- RBM15 exerts myocardial protection through stabilizing NAE1 mRNA.

From the ^aDepartment of Cardiology, Zhongshan Hospital, Fudan University, Shanghai, China; ^bShanghai Institute of Cardiovascular Diseases, Shanghai, China; ^cKey Laboratory of Viral Heart Diseases, National Health Commission, Shanghai, China; ^dKey Laboratory of Viral Heart Diseases, Chinese Academy of Medical Science, Shanghai, China; and the ^eInstitutes of Biomedical Sciences, Fudan University, Shanghai, China. *Drs Cheng and Wu contributed equally to this work.

ABBREVIATIONS AND ACRONYMS

AAV9 = adeno-associated virus 9
GO = Gene Ontology
KEGG = Kyoto Encyclopedia of Genes and Genomes
m⁶A = N⁶-methyladenosine
MeRIP-seq = methylated RNA immunoprecipitation sequencing
METTL = methyltransferase-like
MI = myocardial infarction
mRNA = messenger RNA
NAE1 = NEDD8 activating enzyme E1 subunit 1
NRVMs = neonatal rat left ventricle myocytes
NS = normal saline
qPCR = quantitative polymerase chain reaction
RBM15 = RNA binding motif protein 15
si = small interfering
TUNEL = terminal uridine nick-end labeling
WTAP = Wilms tumor 1-associated protein

SUMMARY

RNA-binding proteins play multiple roles in several biological processes. However, the roles of RBM15—an important RNA-binding protein and a significant regulator of RNA methylation—in cardiovascular diseases remain elusive. This study aimed to investigate the biological function of RBM15 and its fundamental mechanisms in myocardial infarction (MI). Methylated RNA immunoprecipitation sequencing was used to explore the N⁶-methyladenosine (m⁶A) difference between MI and normal tissues. Our findings showed the elevated level of m⁶A in MI, and its transcription profile in both MI and normal tissues. RBM15 was the main regulator and its overexpression attenuated apoptosis in cardiomyocytes and improved cardiac function in mice after MI. Then, we used one target NEDD8 activating enzyme E1 subunit and its inhibitor (MLN4924) to investigate the impact of RBM15 targets on cardiomyocytes. Finally, the enhanced m⁶A methylation in the presence of RBM15 overexpression led to the increased expression and stability of NEDD8 activating enzyme E1 subunit. Our findings suggest that the enhanced m⁶A level is a protective mechanism in MI, and RBM15 is significantly upregulated in MI and promotes cardiac function. This study showed that RBM15 affected MI by stabilizing its target on the cell apoptosis function, which might provide a new insight into MI therapy.

(J Am Coll Cardiol Basic Trans Science 2024;9:631-648) © 2024 The Authors. Published by Elsevier on behalf of the American College of Cardiology Foundation. This is an open access article under the CC BY-NC-ND license (<http://creativecommons.org/licenses/by-nc-nd/4.0/>).

Coronary heart disease, leading to myocardial infarction (MI), is a major contributor to morbidity and mortality on a global scale.¹ In the United States, severe ischemia and loss of cardiomyocytes cause nearly 735,000 annual incidences of irreversible tissue damage, resulting in hypertrophy, ventricular remodeling, dilatation, and heart failure.² After the ischemic injury, the myocardium undergoes a sequence of molecular and cellular interactions after different stages of tissue repair.³ The pathophysiology and pathogenesis of MI are complex and diverse, mainly including the production of reactive oxygen species, apoptosis, autophagy, inflammatory response, mitochondrial dysfunction, and immune response.⁴ Some useful clinical biomarkers and key molecules for MI diagnosis, including NPPB, TNNT2, ANGPT2, and THBS2, have been identified already.⁵⁻⁹ Although advances in MI treatment, such as stem cell therapies, have improved the prognosis of MI, patients with extensive myocardial injury are still at a high risk of chronic heart failure.¹⁰⁻¹² In recent years, multiple studies have found that epigenetic regulation is not only involved in the progression of cardiac hypertrophy, hypertension, heart failure, and other cardiovascular diseases, but also plays an important role in MI.¹³

Epigenetics refers to the heritable changes in the phenotype when the DNA methylation, histone modification, noncoding RNAs, and N⁶-methyladenosine (m⁶A) methylation occur on. An essential epigenetic change known as m⁶A takes place when the adenosine base is methylated at the N⁶ position.^{14,15} Evidence has shown that m⁶A-related proteins play a critical role in diverse biological functions, especially in the development and progression of diseases, such as in promoting gastric cancer progression, inhibiting pancreatic cancer tumorigenesis, or promoting proliferation and tumorigenicity of endometrial cancer.¹⁶⁻¹⁸ Consistent with its roles, m⁶A is emerging as an important pathway mediating cardiovascular diseases.¹⁹⁻²¹ Significant functions are performed by regulators of m⁶A, the most common kind of RNA modification. These functions include destruction, translation, localization, transportation, and RNA processing.^{22,23} The m⁶A RNA editing was discovered in the 1970s and has recently emerged as a significant regulator in gene expression.^{24,25} It is a dynamic and reversible modification mechanism, and its biological functions are mediated through m⁶A-related proteins, named “writer,” “eraser,” and “reader.”²⁶ The formation of m⁶A was modulated by 3 categories of proteins: 9 readers (CBLL1, RNA binding motif protein 15

The authors attest they are in compliance with human studies committees and animal welfare regulations of the authors' institutions and Food and Drug Administration guidelines, including patient consent where appropriate. For more information, visit the [Author Center](#).

Manuscript received January 30, 2023; revised manuscript received January 26, 2024, accepted January 26, 2024.

[RBM15]B, RBM15, ZC3H13, VIRMA, WTAP, METTL16, METTL14, and METTL3), 2 erasers (ALKBH5 and FTO), and 15 readers (IGF2BP1, ELAVL1, RBMX, IGFBP3, IGFBP2, IGFBP1, HNRNPA2B1, LRPPRC, FMR1, HNRNPC, YTHDF3, YTHDF2, YTHDF1, YTHDC2, and YTHDC1).²³ The methyltransferase complex includes methyltransferase-like 3 (METTL3), METTL14, and Wilms tumor 1-associated protein (WTAP) plays an important role on the cardiac function after MI.²⁷ However, there is less research about other methylation regulators, such as RBM15. Therefore, in the present research, we investigated the role of RBM15 in the incidence and progression of MI and provided a novel insight toward myocardial protection.

RBM15 is an RNA-binding protein that can alternatively splice c-Mpl messenger RNA (mRNA) to influence the process of acute megakaryocytic leukemia.²⁸ Moreover, RBM15 is a methylation regulator, although it is named m⁶A methylase, the real function of adding m⁶A is from METTL3.^{29,30} Thus, we investigated whether the role of RBM15 in myocardial protection is significant and whether it could regulate m⁶A process in MI. In this regard, we found that MI tissues exhibited much higher m⁶A methylation levels compared with normal myocardium tissues. The expression of RBM15 was substantially upregulated among m⁶A-related proteins. The developmental expression of RBM15 decreased cell apoptosis both in vitro and in vivo. Then, m⁶A-seq characterization of MI tissues revealed that RBM15 regulated a target gene NEDD8 activating enzyme E1 subunit 1 (NAE1) involving the p53 signaling pathway. Moreover, the expression of NAE1 decreased apoptosis via the mechanism of increased m⁶A methylation. Taken together, these results characterize RBM15 as a significant factor attenuating the apoptosis of cardiomyocytes under MI.

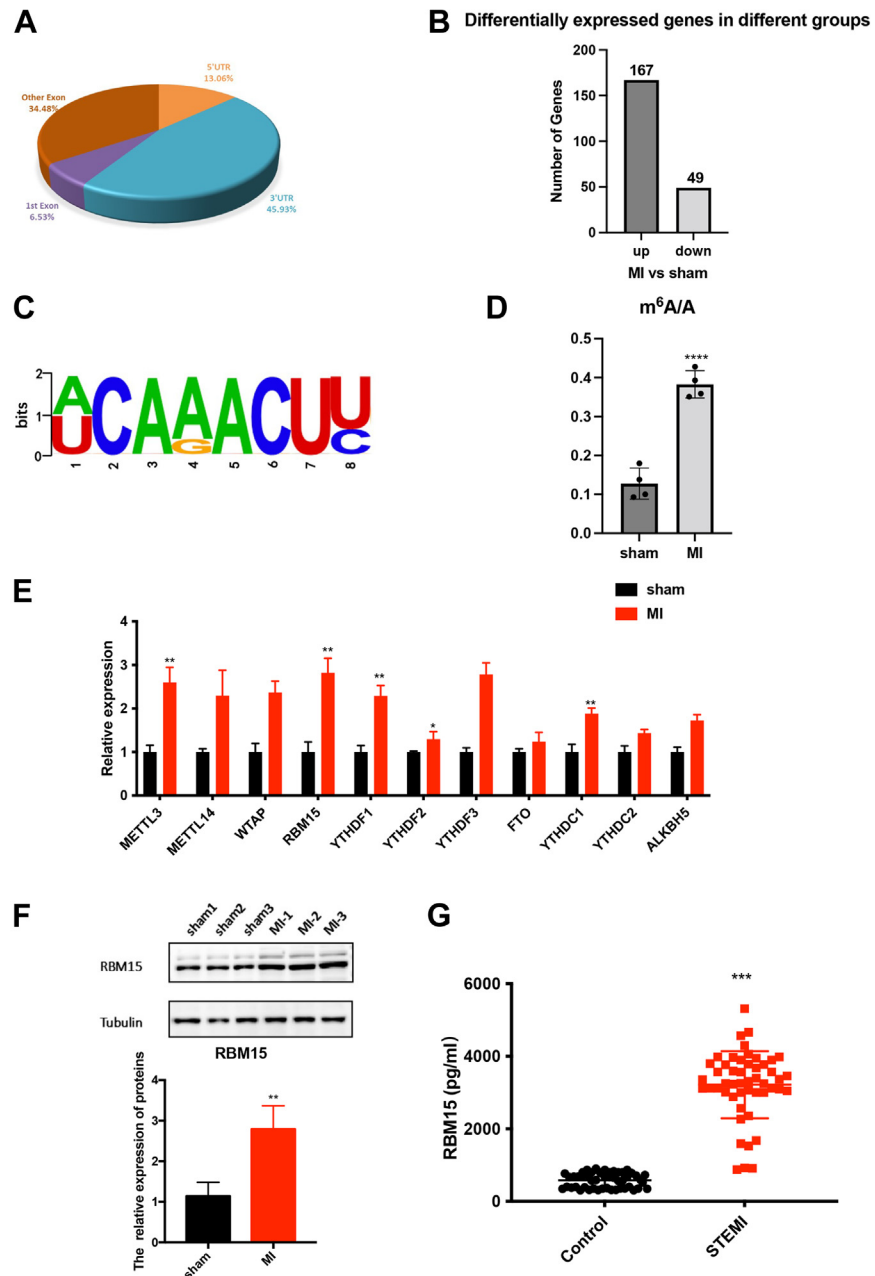
METHODS

HUMAN INCLUSION AND EXCLUSION CRITERIA. In this study, patients with ST-elevation MI who underwent emergent percutaneous catheter interventions in the catheter room of Zhongshan Hospital Affiliated with Fudan University from January 2019 to June 2022 were selected as the experimental group, and healthy individuals matched with the age of the experimental group were selected as the control group (Supplemental Table 1). Blood sample collection and experiments were approved by the hospital ethics committee. The inclusion criteria of experimental group and control groups are as follows. 1) The experimental group standard was a male, 18 to 70 years old with obvious pain symptoms in the

anterior chest area were. The time was >30 minutes, rest or sublingual nitroglycerin cannot alleviate the pain, which may be accompanied by nausea and vomiting; electrocardiography showed elevated ST-segment in 2 (or more) leads, pathological Q-wave, or dynamic change; new left bundle branch block; cardiac troponin T, cardiac troponin I, or creatine kinase-myocardial band increase (>99% of the upper limit of the normal reference range); angiography showed coronary stenosis of >70%; chest pain time of <12 hours; no recent history of infectious diseases, malignant tumors, and so on; and informed consent has been signed. 2) The control group standard was a male, age 18 to 70 years with no chest pain caused by physical labor or excitement. There was no significant change in electrocardiography under normal conditions; cardiac troponin T, cardiac troponin I, or creatine kinase-myocardial band are normal; no recent history of infectious diseases or malignant tumors; and informed consent has been signed.

QUANTIFICATION OF mRNA METHYLATION WITH m⁶A-IMMUNOPRECIPITATION AND QUANTITATIVE POLYMERASE CHAIN REACTION. The m⁶A modification level of a gene was assessed using the Magna methylated RNA immunoprecipitation (MeRIP) Kit (Millipore, cat. #CR203146). For this purpose, cells were collected, double-washed with ice-cold PBS, and centrifuged at a centrifugation rate of 1,500 rpm for 5 minutes at 4 °C. Then, the supernatant was discarded, and the cells were mixed with RIP lysis buffer (100 µL) and incubated on ice for 5 minutes. The obtained cell preparation was stocked at -80°C for future analysis. Then, the m⁶A antibody (8 µg) was added to a tube containing magnetic beads, which was then subjected to rotation at room temperature for 30 minutes. Antibody-coated beads were double-washed with RIP buffer and resuspended in RIP buffer (900 µL) mixed with cell lysate (100 µL), followed by centrifugation at 14,000 rpm for 10 minutes at 4 °C and rotation at 4 °C overnight. Subsequently, the beads were again washed with a high-salt buffer, and RNAs were extracted with RIP wash buffer. Finally, the RNA enrichment analysis was performed by quantitative polymerase chain reaction (qPCR).

METHYLATED RNA IMMUNOPRECIPITATION SEQUENCING LIBRARY CONSTRUCTION AND SEQUENCING. For this purpose, total RNA extraction was performed by TRIZOL reagent (Invitrogen) and was quantified by Bioanalyzer 2100 and RNA 6000 Nano LabChip Kit (Agilent) with the RIN number more than 7.0. Then, almost 200 µg of the total RNA was used for the purpose of isolating and purifying the poly(A) mRNA with poly(T) oligonucleotides content attached to the

FIGURE 1 MeRIP-seq Analysis Unveiling the m⁶A Profiles in the MI

(A) There were different peaks between MI and sham samples. (B) The differentially expressed genes were targeted by m⁶A modification in MI and sham groups. (C) The m⁶A consensus sequence motif was identified in NRVMs. (D) The total m⁶A level was increased in MI. (E) Relative m⁶A-related proteins increased in MI. (F) The protein expression of RBM15 increased notably in MI. (G) The RBM15 quantification of serum from patients with STEMI and the healthy individuals, as assessed by ELISA. (n = 50). Data are presented as mean ± SEM. **P* < 0.05, ***P* < 0.01, ****P* < 0.001. In data D, E, and F, differences were compared between sham and MI. In data G, difference was compared between controls and STEMI. All data were analyzed using unpaired Student's *t* test. ELISA = enzyme-linked immunosorbent assay; m⁶A = N⁶-methyladenosine; MI = myocardial infarction; MeRIP-seq = methylated RNA immunoprecipitation sequencing; STEMI = ST-segment elevation myocardial infarction.

magnetic beads (Invitrogen). Then, the poly(A) mRNA fractions were fragmented into ~100-nt-long oligonucleotides using divalent cations at an elevated temperature. The RNA fragments were then filtered and subjected to incubation with an m⁶A-specific antibody (No. 202003, Synaptic Systems) in immunoprecipitation buffer (50 mM Tris-HCl, 750 mM NaCl, and 0.5% Igepal CA-630) supplemented with 0.5 μg/μL bovine serum albumin at 4 °C. After 2 hours, the RNA-antibody mixture was further incubated with protein-A beads. Moreover, RNA was washed with elution buffer (1 × immunoprecipitation buffer and 6.7 mM m⁶A) and precipitated using ethanol (75%). The immunoprecipitation fragments containing m⁶A and untreated input control fragments were converted to the final complementary DNA library by means of the deoxyuridine triphosphate method complying with strand-specific library preparation. The average insert size for the paired-end libraries was ~100 ± 50 bp. Finally, an Illumina Novaseq 6000 platform was performed for the paired-end 2 × 150 bp sequencing.

METHYLATED RNA IMMUNOPRECIPITATION SEQUENCING DATA ANALYSIS. First, Cutadapt and Perl scripts were used for the quality control of the reads to remove the adaptor, low-quality bases, and undetermined bases.³¹ HISAT2 was used for the purpose of mapping reads to the genome with default parameters.³² The m⁶A peaks were obtained by the R package exomePeak.³³ The peak annotation was done with gene architecture by ChIPseeker.³⁴ Then, StringTie was performed to measure the expression levels for all mRNAs from input libraries by calculating the fragments per kilobase of transcript per million mapped reads.³⁵ Finally, the differentially expressed mRNAs with a fold-change of 2 and a *P* value of <0.05 were selected with the aid of the edgeR package in R.³⁶

QUANTIFICATION AND STATISTICAL ANALYSIS. All data are shown as mean ± SEM. All statistical analyses, unless otherwise indicated, were performed by GraphPad Prism 9.0 (GraphPad Software). Statistical significance was calculated by 2-tailed unpaired Student's *t* test if 2 independent groups were compared. One-way analysis of variance was used for comparisons among multiple groups. Post hoc analyses were performed using Holm-Sidak's post hoc test for multiple pairwise comparisons or by controlling the false discovery rate using the method of Benjamini, Krieger, and Yekutieli. Kaplan-Meier survival analysis was used to reveal the survival rate of each group in vivo. *P* values of <0.05 were considered statistically significant (**P* < 0.05, ***P* < 0.01, ****P* < 0.001). The

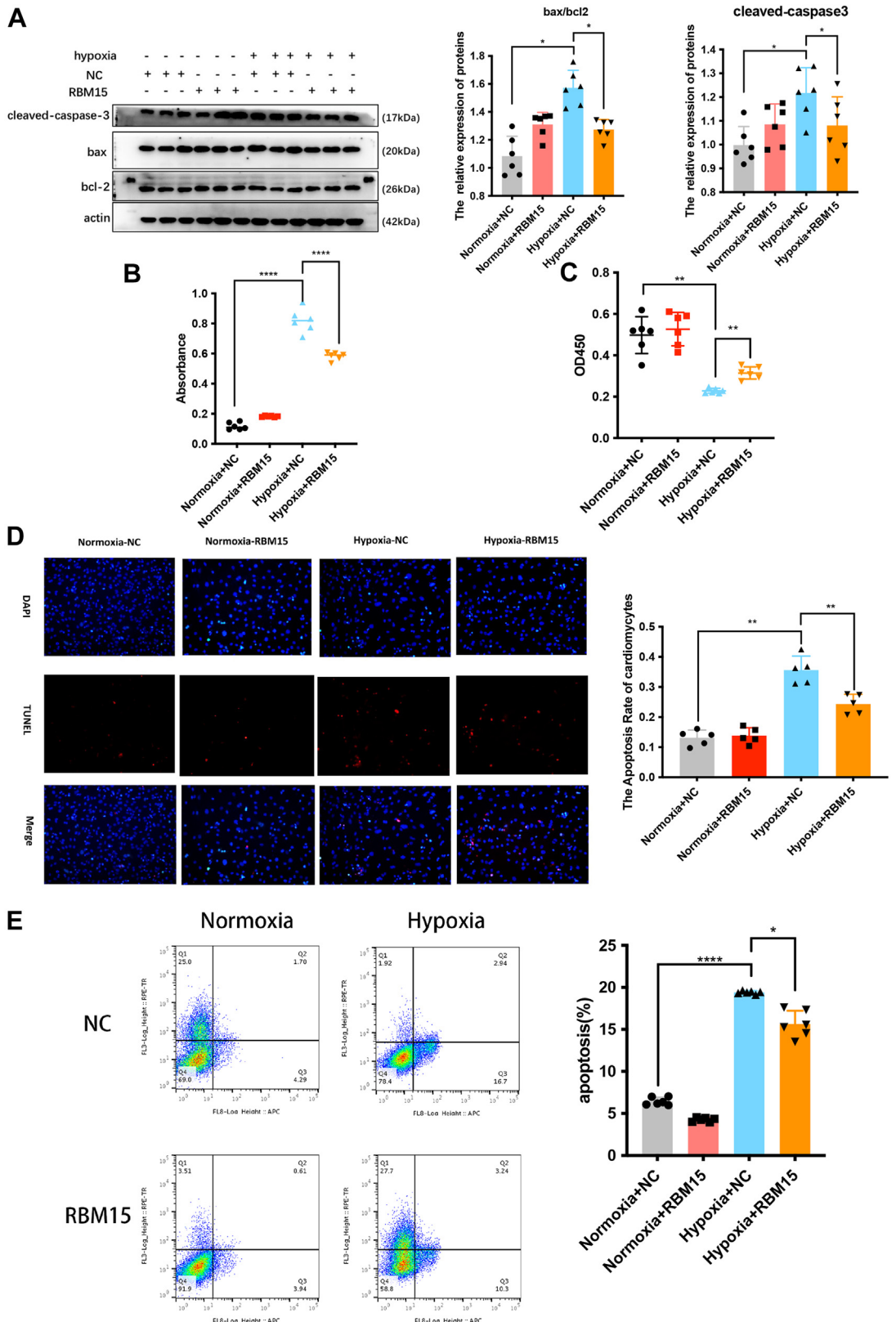
significant threshold in multiple tests were set by a false discovery rate of <0.05.

RESULTS

HIGHLY EXPRESSED m⁶A-RELATED PROTEIN RBM15 IN MI. To study the presence of the m⁶A modification during MI, we successfully constructed mice models of MI. We confirmed the occurrence of the m⁶A modification during the MI process by methylated RIP sequencing (MeRIP-Seq); specifically, 1,538 m⁶A peaks were observed in MI compared with the control, and 45.93% of the m⁶A peaks occurred in the 3' untranslated region (Figure 1A). We found 167 upregulated genes and 49 downregulated genes (Figure 1B). In total, the m⁶A sequence identified that 397 transcripts were upregulated, while 252 transcripts were downregulated (Supplemental Figure 1A). Gene Ontology (GO) analysis showed that the differentially expressed m⁶A-related transcripts were enriched in gene sets involved in extracellular space, extracellular matrix, and positive regulation of apoptosis cell clearance, revealing that m⁶A regulation might have an impact on apoptosis (Supplemental Figure 1B). Moreover, Kyoto Encyclopedia of Genes and Genomes (KEGG) analysis showed that the differentially expressed m⁶A-related transcripts were involved in histidine metabolism, hypoxia-inducible factor-1 signaling pathway, complement and coagulation cascades, and extracellular matrix-receptor interaction (Supplemental Figure 1C). When mapping the m⁶A methylomes, the m⁶A consensus sequence RRACH motif was identified to be highly enriched within m⁶A sites in the immunopurified mRNA (Figure 1C).

Furthermore, an elevated total m⁶A mRNA level was identified in MI (Figure 1D). Then, the expressions of m⁶A-related proteins such as some "writers" (METTL3, METTL14, WTAP and RBM15), "erasers" (FTO and ALKBH5), and "readers" (YTHDF1, YTHDF2, YTHDF3, YTHDC1, and YTHDC2) in MI tissues were assessed with qPCR (Figure 1E). The expression of METTL3 and RBM15 increased dramatically in MI among other methylase-related proteins (Figure 1E). Because we have investigated the role of METTL3 in MI, in this research we paid attention to RBM15. Then, we assessed the protein expression of RBM15 by Western blotting, which also showed a highly elevated expression level in MI tissues (Figure 1F). To investigate potential diagnosis or treatment roles of RBM15 in a clinical context, we examined serum from patients with ST-segment elevation MI and healthy individuals using enzyme-linked immunoassay. Finally, we observed that the RBM15 level increased

FIGURE 2 The Protection of Targeting RBM15 on the Cardiomyocytes Under Hypoxia



remarkably (Figure 1G). To imitate the MI circumstances, neonatal rat left ventricle myocytes (NRVMs) under hypoxia conditions at different time points (1, 3, 6, 12, and 24 hours) were set to assess the expression of RBM15; we found the highly elevated expression level after 3 hours (Supplemental Figure 1D). These results proved that RBM15 might have an important role in the m⁶A modification in MI.

THE EFFECTS OF OVEREXPRESSING RBM15 ON CARDIOMYOCYTES UNDER HYPOXIA. To investigate the biological roles of RBM15 in cardiomyocytes, RBM15 silencing and overexpression were established via transfection into NRVMs (Supplemental Figures 2A to 2D). Subsequently, loss- and gain-of-function assays were carried out for the purpose of identifying the role of RBM15 in NRVMs under hypoxic conditions. Considering the key role of bcl-2, cleaved-caspase3, and bax in mediating apoptosis, Western blotting analysis confirmed that RBM15 overexpression attenuated apoptosis activity of NRVMs when treated in hypoxic conditions (Figure 2A). Furthermore, lactate dehydrogenase release assays showed that RBM15 overexpression also decreased apoptosis of NRVMs (Figure 2B). The results from the CCK8 assay also suggested that RBM15 decreased the apoptosis of NRVMs under hypoxic conditions (Figure 2C). Subsequently, we used a terminal uridine nick-end labeling (TUNEL) assay and flow cytometry to further demonstrate the protective effect of RBM15. After hypoxia treatment, there were few TUNEL-positive nuclei in NRVMs that overexpressed RBM15 (Figure 2D). Representative flow cytometry plots were generated for control and NRVMs overexpressing RBM15; they demonstrated a decreased number of apoptotic cells in the RBM15-overexpressing treated group (Figure 2E). Hence, those in vitro results showed that RBM15 could ameliorate hypoxia-induced cell death.

APOPTOSIS OF NRVMs WITH SILENCED RBM15 UNDER HYPOXIC CONDITIONS. To further investigate the functional role of RBM15 in NRVMs, we used small

interfering (si)-RBM15 to demonstrate whether the effects of RBM15 knockdown are the opposite from those of RBM15 overexpression. To this end, we performed Western blotting and identified the apoptosis-related markers including bax/bcl-2 and cleaved-caspase3. We found that the RBM15 knockdown remarkably promoted NRVMs apoptosis following hypoxia (Figure 3A). Similar to the Western blotting results, the lactate dehydrogenase release assay and CCK8 assay showed that RBM15 silencing increased cell death (Figures 3B and 3C). The TUNEL assay and flow cytometry showed the same results, indicating that RBM15 knockdown promoted NRVMs apoptosis after hypoxic treatment (Figures 3D and 3E).

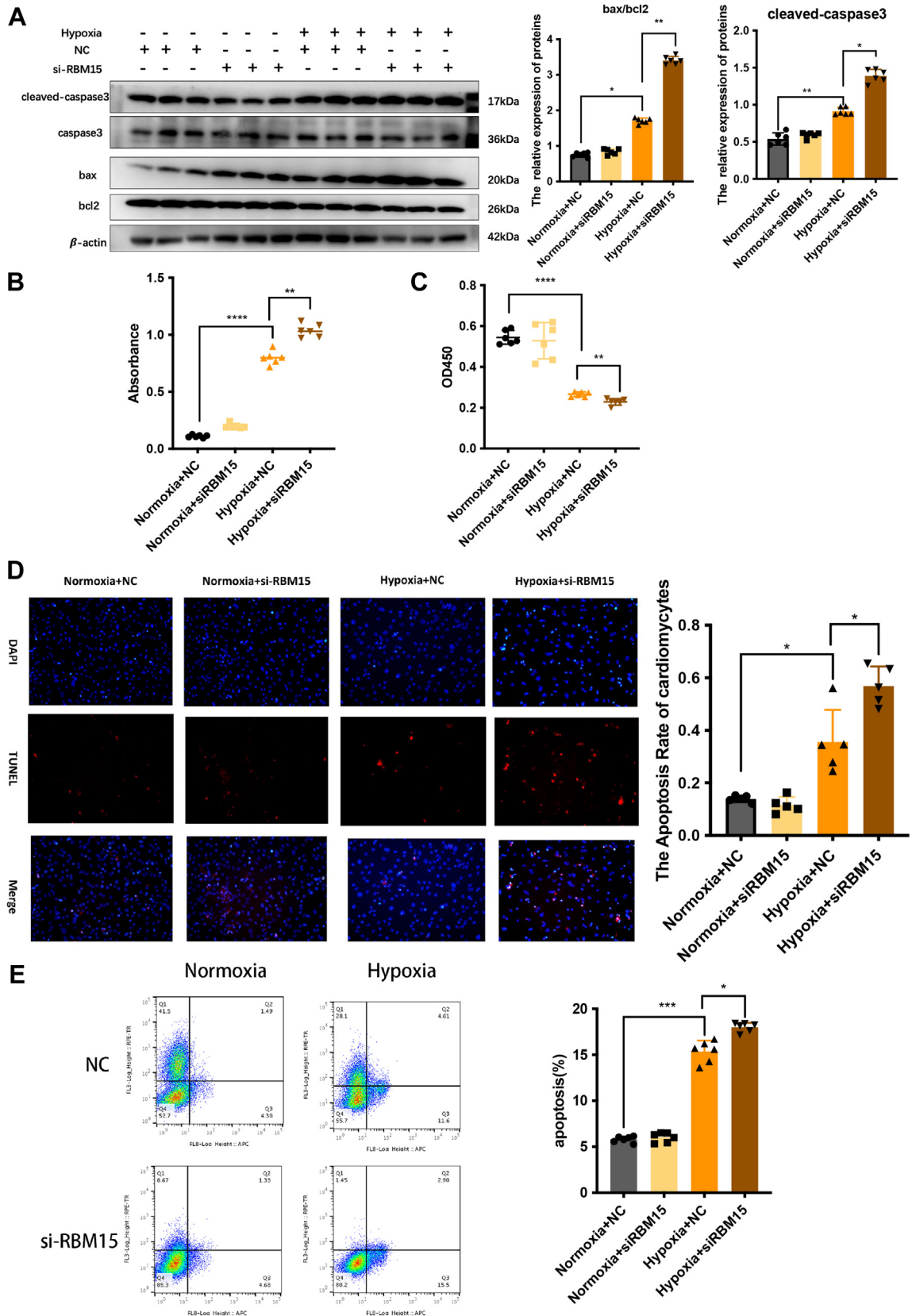
IMPROVED HEART FUNCTION AND ATTENUATED CARDIAC FIBROSIS AFTER OVEREXPRESSING RBM15. The protective effects of RBM15 overexpression in cells under hypoxia allowed us to further analyze its effect on the infarction-induced cardiac dysfunction. Then, we successfully established the mouse MI model overexpressing RBM15 (Supplemental Figures 2E and 2F). Given that glycogen consumption can cause hypoxia- and glycolysis-induced damage of NRVMs at the very beginning of MI, apoptosis was assessed through Western blot and TUNEL assays on the infarcted tissues and remote areas. We found that, 1 week after MI, the expression levels of cleaved-caspase3 and bax significantly decreased, whereas the expression level of bcl-2 increased in the RBM15-Adeno-associated virus 9 (AAV9) group (Figures 4A to 4F). The TUNEL assay showed that the number of TUNEL-positive nuclei in the RBM15-AAV9 group was lower than that of the NC-AAV9 group (Figure 4G). Thus, the in vivo results showed that RBM15 was able to ameliorate MI-induced cell death.

At weeks 1, 2, and 4 after MI, serial echocardiography and hemodynamic measurements were used to evaluate the cardiac function in mice from the indicated groups. We found that the cardiac function was improved by RBM15 overexpression, as indicated by

FIGURE 2 Continued

(A) The apoptosis markers cleaved-caspase3 and bax, and the antiapoptotic marker bcl-2 were assessed by Western blotting (left); the relative ratios of cleaved-caspase3 and bax/bcl-2 protein levels were calculated based on Western blotting results (middle and right). (B, C) Cell injury was determined by the LDH release assay and CCK8 assay (n = 6). (D) Representative images of TUNEL staining of NRVMs for DNA de-fragmentation showing the apoptotic cells (nuclei stained in blue with DAPI, apoptotic cells stained in red) (left) (n = 5). Statistical results of TUNEL-positive cells per field indicated that RBM15 decreased treatment-induced cell apoptosis (right). (E) The representative images of flow cytometry using APC and 7-AAD staining (left); statistical analysis of apoptosis ratio of the flow cytometry data (right) (n = 6). Scale bar, 100 μm. n = 3. Data are presented as mean ± SEM. *P < 0.05, **P < 0.01, ****P < 0.0001. In data A (right), B, C, D (right), and E (right), differences were compared between Normoxia + NC, Hypoxia + NC, and Hypoxia + RBM15. All data were analyzed using One-way analysis of variance followed by Tukey's post hoc analysis. DAPI = 4',6-diamidino-2-phenylindole; LDH = lactate dehydrogenase; NC = normal control; NRVM = neonatal rat left ventricle myocyte; TUNEL = terminal uridine nick-end labeling.

FIGURE 3 Apoptosis of NRVMs With Silenced RBM15 Under Hypoxic Conditions



higher EF%, FS% and lower LVIDd, LVIDs at week 4 after MI (Figures 5A to 5E, Supplemental Figures 3A to 3E, Supplemental Table 5). The effects of RBM15 on the post-MI outcomes were further confirmed by assessing smooth muscle/collagen through Masson staining. The smooth muscle/collagen ratio in the normal saline (NS) group was considerably lower than that in the sham group (Figures 5F and 5G). Furthermore, hematoxylin and eosin staining was performed to evaluate the cell morphology of the myocardium. For example, the cardiomyocytes were arranged regularly in the sham group, showing obvious nuclei and no inflammatory cell infiltration. In contrast, the MI, MI with NS, and MI with NC-AAV9 groups displayed major myocardial cell necrosis, disordered myocardial fiber arrangement, and quantities of inflammatory cell infiltrations. The cardiomyocytes in MI within the RBM15-AAV9 group showed a much more orderly arrangement with a remarkable reduction in the range and degree of cell necrosis (Figure 5H). Finally, the probability of survival of each group was analyzed and showed that the mortality rate of mice with injection RBM15 after MI was decreased at the final point (Figure 5I, Supplemental Table 6). Taken together, these in vivo data indicated that RBM15 dramatically decreased infarction and improved cardiac function.

ANALYSIS OF DOWNSTREAM TARGETS OF RBM15 IN CARDIOMYOCYTES. To investigate downstream targets of RBM15, the precise mechanisms of the observed RBM15-dependent phenotypes were further investigated with the aid of an integrated combined MeRIP-seq and RNA-seq. MeRIP-seq revealed 1,538 differential m⁶A peaks with increased abundance, whereas RNA-seq uncovered 851 upregulated transcripts (Supplemental Tables 7 and 8). We focused more on oncogenes whose methylation and expression profiles were regulated by RBM15. Thus, only those transcripts that had both hypo-m⁶A peaks and elevated expression levels upon RBM15 over-expression were considered. All differentially

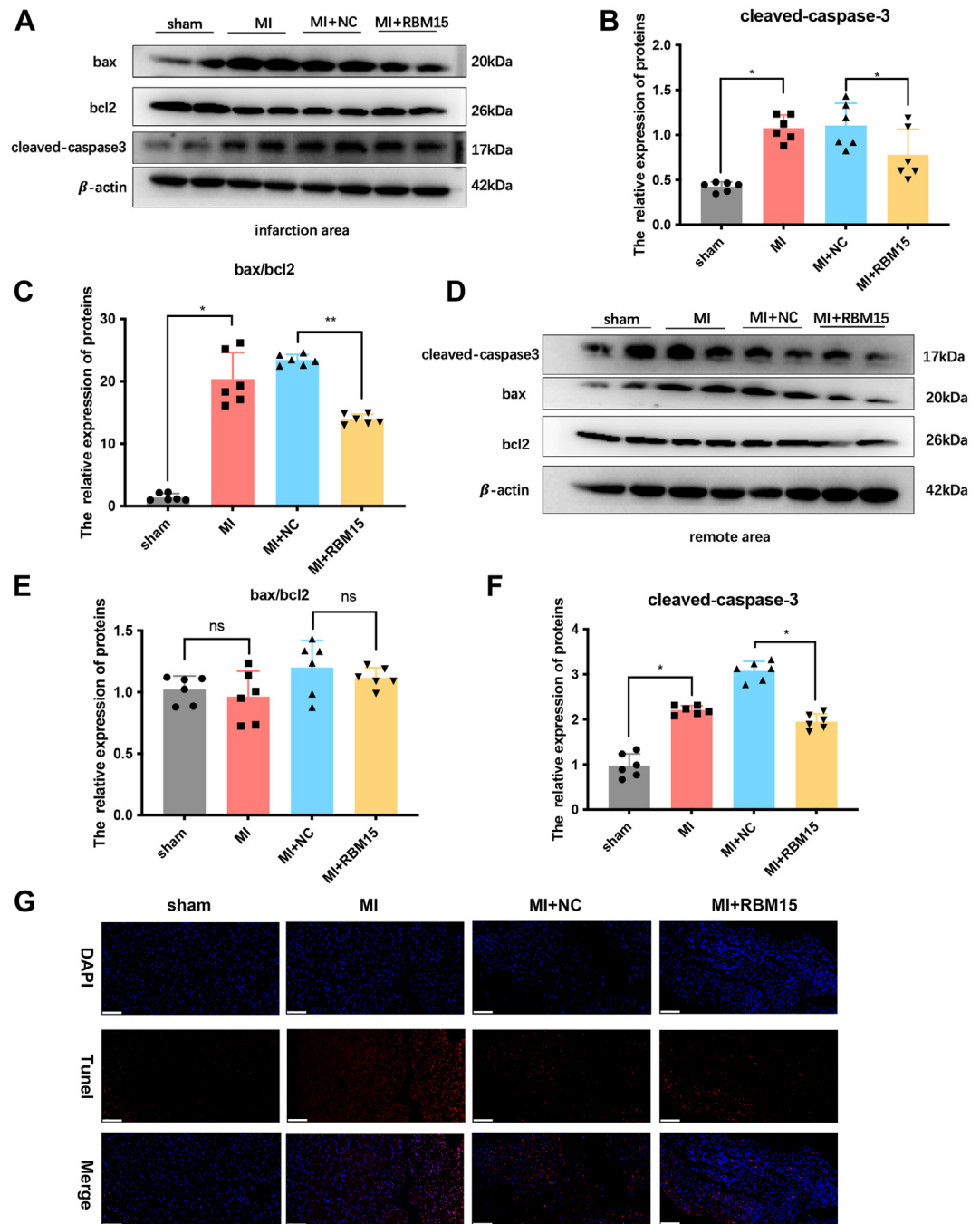
expressed gene fold changes are shown in Figure 6A. Then, we conducted the enrichment analysis of all the RBM15-upregulated genes into GO term annotation. The top 10 enrichment GO terms are shown in Figure 6B, and we found that gene sets were mainly involved in iron-sulfur cluster assembly, negative regulation of phosphorylation, and regulation of apoptosis process. Moreover, we performed text mining to find any relationship between MI and the significantly enriched GO terms. For example, it has been reported that the ischemic-reperfusion injury results in oxidative damage led by cysteine ligands of the iron-sulfur cluster.³⁷ In MI, PPM1L could inhibit IKKβ's phosphorylation and activation by binding to it, thereby leading to the impairment of nuclear factor κB signaling activation and inflammatory suppression.³⁸

To further systematically screen biological functions, we searched for all differentially expressed genes in the protein-protein interaction network (Figure 6C). Each protein cluster is shown in a distinct color, and the cluster enrichment function is labeled in the corresponding colored boxes. Moreover, KEGG analysis showed that localization, immune response, and metabolic process were related to the RBM15 regulation process (Figure 6D). Importantly, filtering the 1538 increased m⁶A peaks with the 851 upregulated genes resulted in the identification of 25 genes (Figure 6E). Among these 25 genes, we chose one of the highly conserved genes, named NAE1, in the regulation of the apoptotic process to investigate the details of the regulation (Supplemental Figures 4A and 4B).

ENHANCED NAE1 EXPRESSION BY RBM15 THROUGH STABILIZING ITS mRNA. To demonstrate whether RBM15 regulates NAE1 mRNA, we first found that the NAE1 mRNA expression level increased dramatically in the infarction area in the MI model (Figure 7A), and its level decreased after silencing RBM15 in NRVMs under hypoxic conditions (Figure 7B). In contrast, NAE1 mRNA expression level increased dramatically

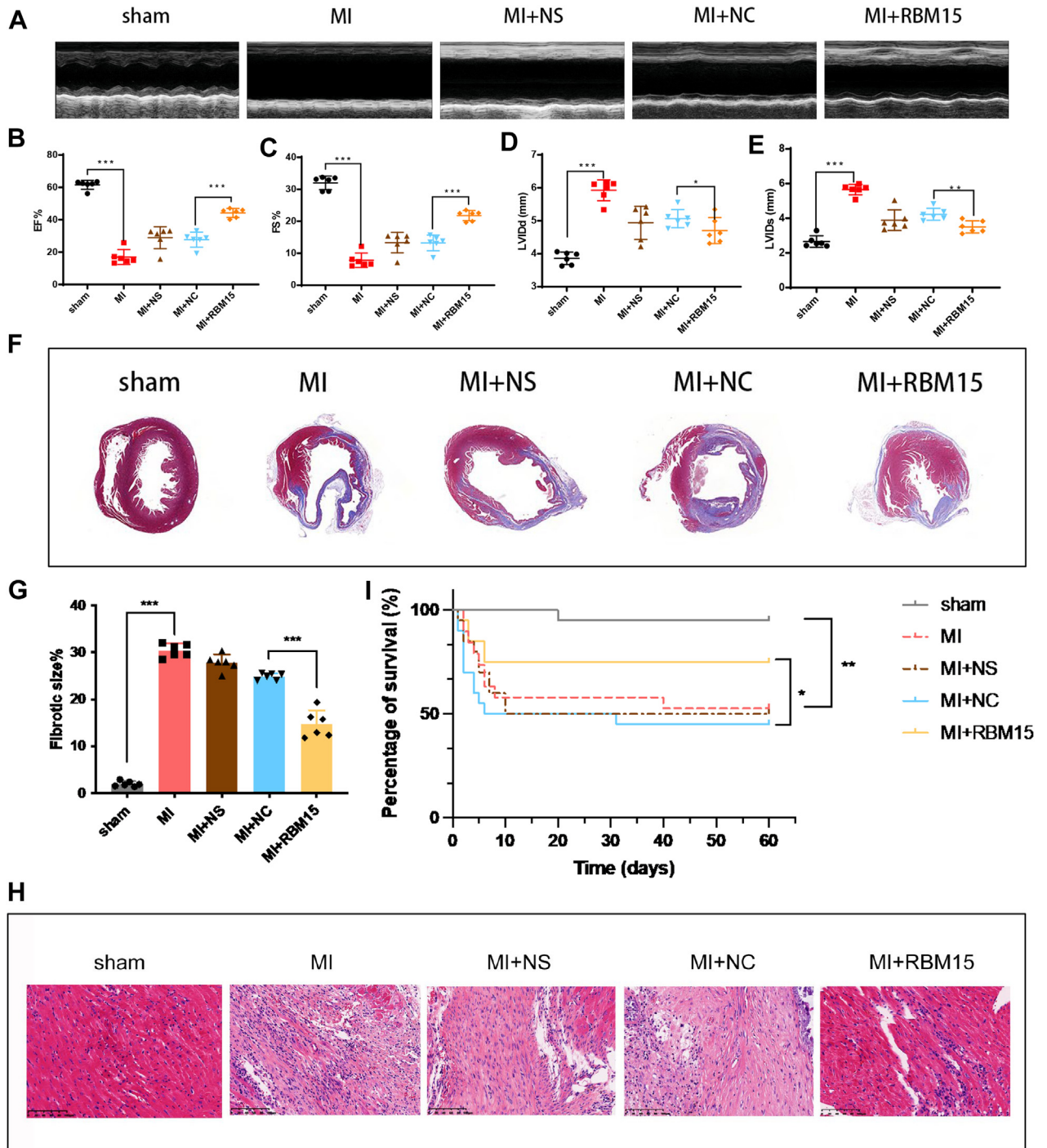
FIGURE 3 Continued

(A) The apoptosis marker bax and the anti-apoptosis marker bcl-2 were assessed by Western blotting (left); the relative ratio of bax/bcl2 protein levels was calculated (middle and right). (B, C) The LDH release assay and CCK8 assay were used to elucidate the cell injury. (B) LDH release assay, (C) CCK8 assay (n = 6). (D) Representative images of TUNEL staining of NRVMs for DNA defragmentation showing the apoptotic cells (nuclei stained in blue with DAPI and apoptotic cells stained in red) (left). Statistical results of TUNEL-positive cells per field indicated that RBM15 decreased treatment-induced cell apoptosis (right) (n = 5). (E) The representative images of flow cytometry using APC and 7-AAD staining (left); statistical analysis of apoptosis ratio of the flow cytometry data (right) (n = 6). Scale bar, 100 μm. n = 3. Data are presented as mean ± SEM. * P < 0.05, ** P < 0.01, *** P < 0.001. In data A (right), B, C, D (right), and E (right), differences were compared between Normoxia + NC, Hypoxia + NC, and Hypoxia + si-RBM15. All data were analyzed using one-way analysis of variance followed by Tukey's post hoc analysis. 7-AAD = 7-aminoactinomycin D; APC = allophycocyanin; si-RBM15 = small interfering RBM15; other abbreviations as in Figure 2.

FIGURE 4 Decreased Apoptosis After Injecting RBM15-AAV9 Into the Myocardium after MI

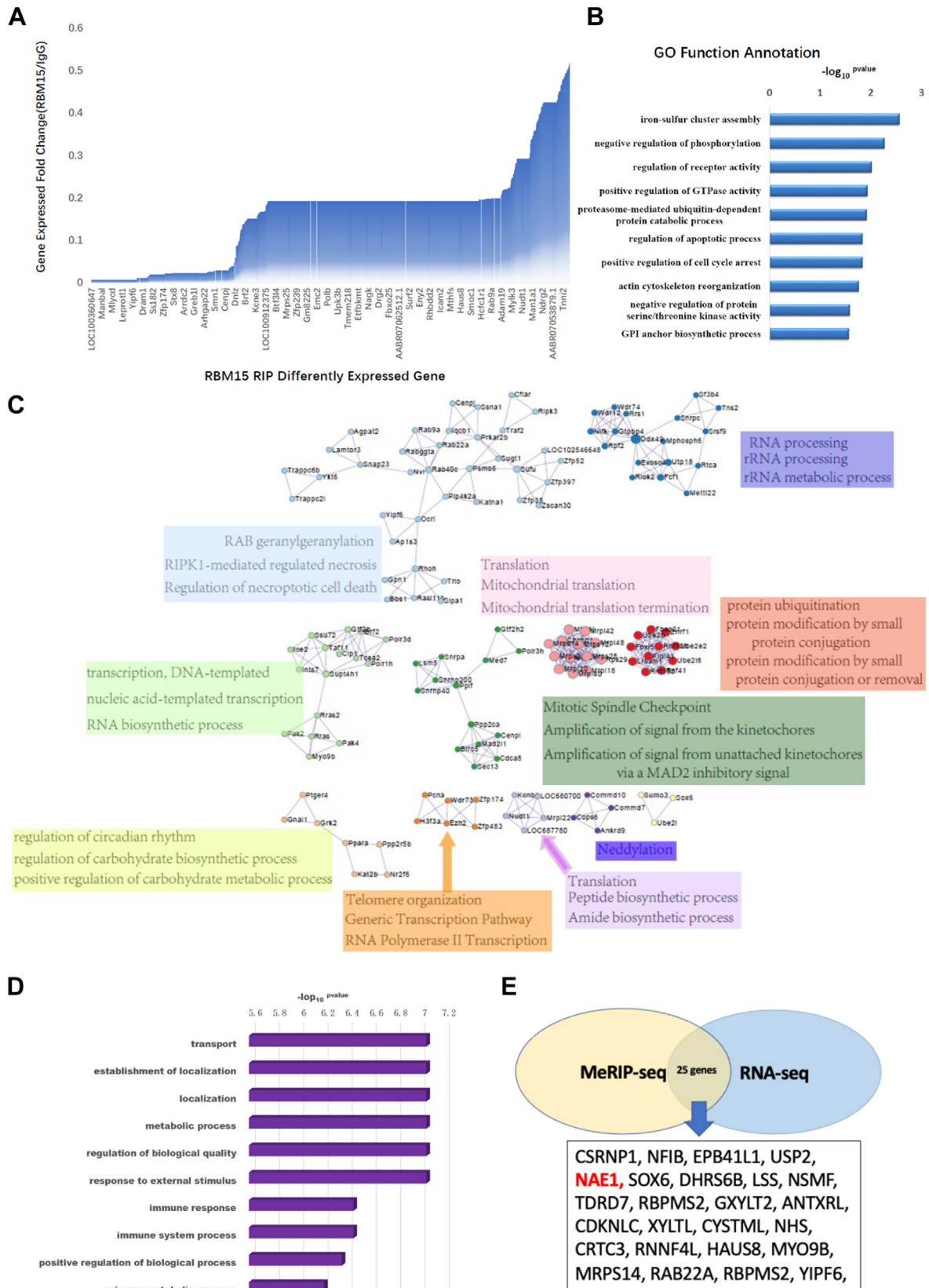
(A to F) The apoptosis markers cleaved-caspase3 and bax, and the anti-apoptosis marker bcl-2 were assessed by Western blotting in the infarct area and remote area, and the relative ratios of cleaved-caspase3, bax/bcl-2 protein levels were calculated. (G) Histochemical identification of TUNEL-positive cells in the post-MI heart on day 7. Infarcted area of TUNEL and DAPI (left) and the rate of TUNEL-positive cells (right) ($n = 6$). Scale bar, 100 μ m. Data are presented as mean \pm SEM. * $P < 0.05$, ** $P < 0.01$, **** $P < 0.0001$. In data B, C, E, F, and G (down), differences were compared between sham and MI, or between MI + NC and MI + RBM15. All data were analyzed using unpaired Student's t test Abbreviations as in [Figures 1 and 2](#).

FIGURE 5 Improved Heart Function and Attenuated Cardiac Fibrosis After Overexpressing RBM15



(A) Representative echocardiography images on week 4 post-MI (n = 6). (B to E) The measurement of left EF%, FS%, LVIDd, and LVISd on week 4 post-MI and NS injection, NC injection, and RBM15 injection. (F) The representative images of Masson's trichrome staining. (G) Percentage of left ventricle area occupied by scar tissue 4 weeks post-MI and NS injection, NC injection, and RBM15 injection, (n = 6). (H) HE staining of myocardial tissue in the marginal zone of MI. Scale bar, 100 μm. (I) MI + RBM15 group showed improved overall survival. Kaplan-Meier curves were generated, log-rank (Mantel-Cox) test (n = 20). Data are presented as mean ± SEM. ***P < 0.001. In data B, C, D, E, G, and I, differences were compared between sham and MI, or between MI + NC and MI + RBM15. All data were analyzed using unpaired Student's *t* test. EF% = ejection fraction %; FS% = fraction shortening %; HE = hematoxylin and eosin; LVIDd = left ventricular internal dimension-diastole; LVISd = left ventricular internal dimension-systole; NS = normal saline; other abbreviations as in [Figures 1 and 2](#).

FIGURE 6 Analysis of Downstream Targets of RBM15 in Cardiomyocytes



after overexpressing RBM15 in NRVMs under hypoxic condition (Figure 7C). To investigate the RNA-binding role of RBM15 in NAE1 mRNA, we performed RIP-qPCR, and found that RBM15 could bind quantities of NAE1 mRNA (Figure 7D). After treatment with actinomycin D (a transcription inhibitor), the qPCR analysis revealed that the expression of NAE1 significantly decreased after silencing RBM15, indicating that RBM15 can maintain the stability of NAE1 (Figure 7E). Taken together, our findings revealed that RBM15 enhanced NAE1 expression via stabilizing its mRNA.

APOPTOSIS OF CARDIOMYOCYTES AFTER INHIBITION OF NAE1. Given that the GO and KEGG analyses showed that NAE1 might be involved in the apoptosis pathway, we further investigated whether NAE1, a downstream target of RBM15, has an effect on cardiomyocyte apoptosis under hypoxia. The role of NAE1 in the protective effect on NRVMs was validated by infecting the cells with adenoviruses expressing NAE1 or siRNA. The Western blotting data proved the upregulated expression of NAE1 and a remarkable decrease in proapoptosis markers (cleaved-caspase3, bax) in NRVMs (Figure 8A). In contrast, we used siNAE1-1 and siNAE1-2 to infect NRVMs, and after hypoxia treatment, we found that the NAE1 knockdown promoted apoptosis of NRVMs (Figure 8B). Furthermore, the lactate dehydrogenase release and CCK8 assays were used to assess the NRVMs apoptosis, and the results indicated that the NAE1 overexpression was able to decrease apoptosis of NRVMs (Figures 8C to 8F). To further examine the proapoptosis effect of the NAE1 knockdown, NRVMs were treated with MLN4924 (the NAE1 inhibitor) at different concentration points. We found that the levels of NAE1 significantly decreased and proapoptosis markers, including cleaved-caspase3 and bax significantly increased (Figure 8G). These data demonstrated that NAE1 inhibition enhanced the death of NRVMs.

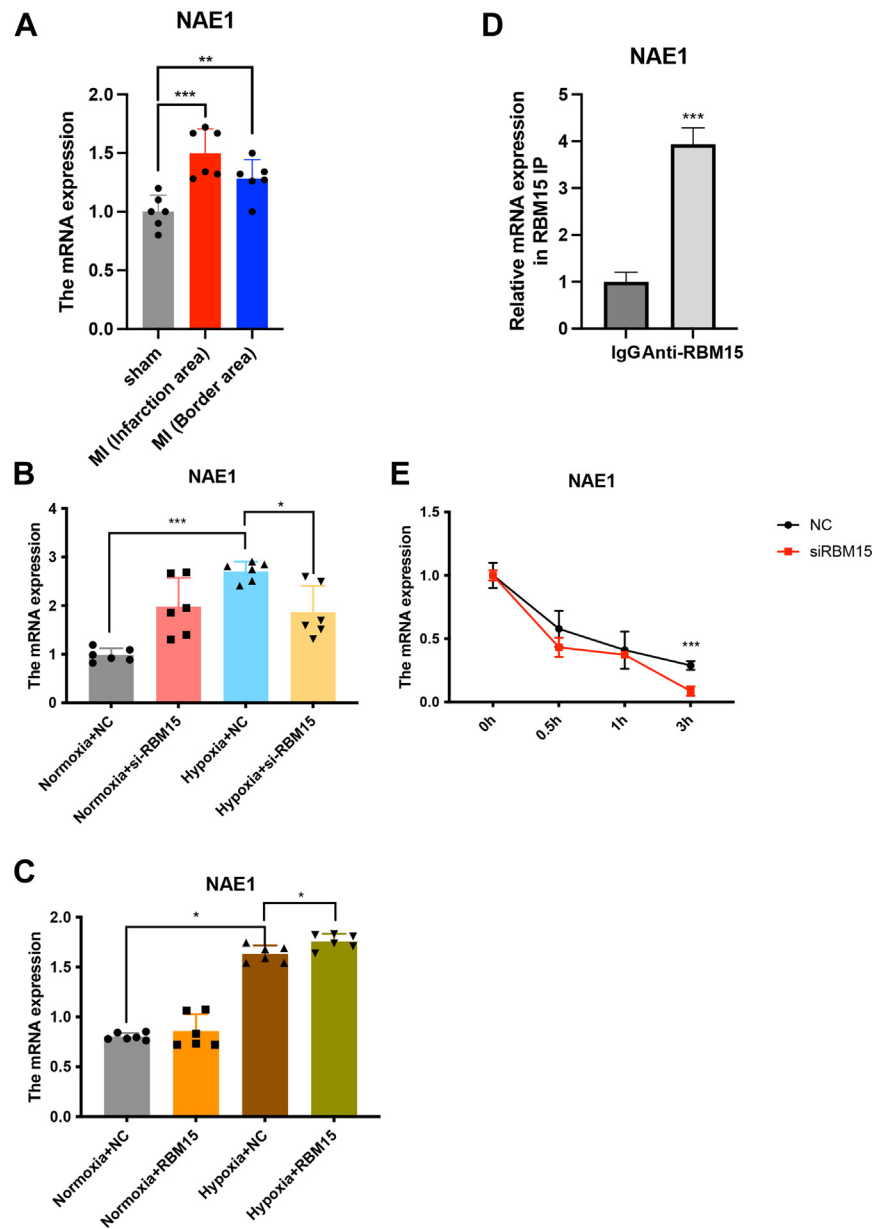
DISCUSSION

Despite significant advances made in early detection and treatment over the course of the last decade, MI

continues to be a primary cause of death and disabilities.³⁹ Many investigators are actively looking for potential markers and investigating the components of immune cell infiltration of MI, both of which have the potential to have a significantly beneficial impact on the long-term survival of patients with MI. Many studies have reported the potential of using mRNA as a potentially useful indicator of diseases in the cardiovascular field, particularly MI. A growing body of data shows that m⁶A regulators exhibit a wide range of regulatory effects on the diversity of biological activity. However, few people have been able to understand the role of m⁶A regulators in MI.⁴⁰ The m⁶A plays a modulatory role in nearly all stages of the RNA life cycle, including mRNA processing, nuclear export, translation modulation, and even the phase separation potential of mRNA.⁴¹⁻⁴³ It has been reported that m⁶A plays an important role in cardiovascular diseases, not only as a biomarker in diagnosis of MI, but also as a medicine in treatment of cardiac remodeling.^{44,45} Shi et al⁴⁴ used comprehensive analysis of m⁶A regulators expression to identify distinct molecular subtypes of MI, and they found several genes were significantly related to the development of MI, with being regulated by m⁶A methyltransferases. In the present research, we also observed the differences in m⁶A modification in MeRIP of MI and sham control tissues. Moreover, RBM15 was screened as a dramatically changed m⁶A-related protein. Given that we have demonstrated METTL3, the main m⁶A methyltransferase regulated the myocardial remodeling after MI, we investigated the role of RBM15 in MI. We found that the expression level of RBM15 was significantly upregulated in MI. The GO analysis and KEGG analysis revealed that many apoptosis-related genes during MI were remarkably regulated by m⁶A. Overexpression of RBM15 decreased the cardiomyocytes' apoptosis. This observation was further corroborated by in vivo findings that the heart function was improved in the MI mice overexpressing RBM15. Later, NAE1—an RBM15 target—was found by filtering MeRIP-seq and RBM15-RIP-seq. We found that RBM15 positively regulated the stability of the target NAE1 mRNA. Notably, similar to RBM15, the overexpression of

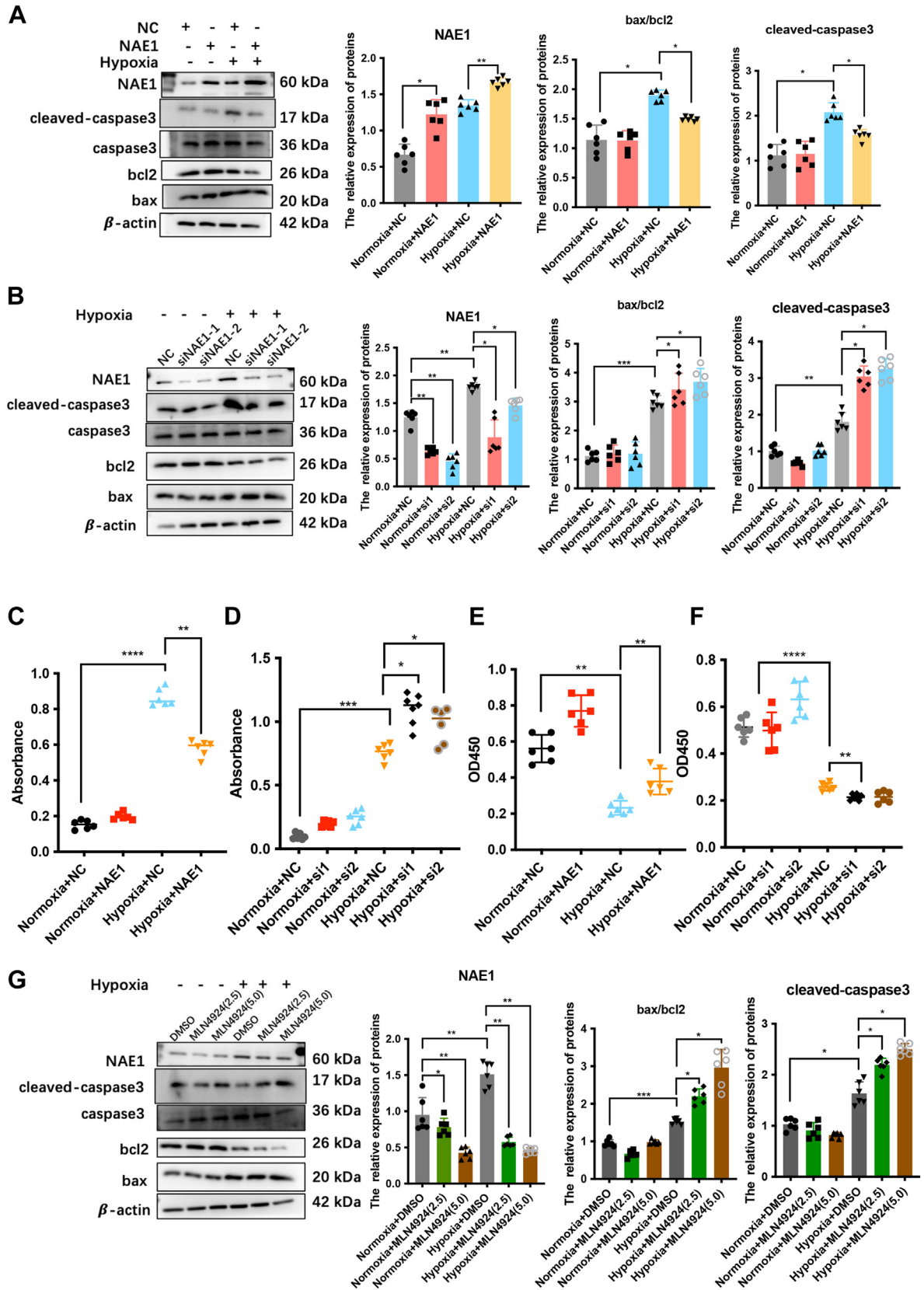
FIGURE 6 Continued

(A) The 851 m⁶A upregulated genes are shown in the bar plot. The x axis indicates the differentially expressed genes, and the Y-axis shows the expression fold change. (B) The top 10 enrichment GO terms of the RBM15-upregulated gene was shown. The y axis indicates the GO terms, the x axis shows the -log P value of enrichment analysis. (C) The protein-protein interaction motifs are shown. The circle node indicates the gene, while the line depicts the interaction between the two proteins. Each colored group of nodes shows a certain motif. The motif function is listed in the corresponding box. (D) The top 10 enrichment KEGG terms of the RBM15-upregulated genes are shown. (E) Filtering the increased genes in MeRIP-seq and RBM15-RIP-seq identified NAE1 as a direct target of RBM15. GO = Gene Ontology; KEGG = Kyoto Encyclopedia of Genes and Genomes; NAE1 = NEDD8 activating enzyme E1 subunit 1; other abbreviations as in Figure 1.

FIGURE 7 Enhanced NAE1 Expression by RBM15 Through Stabilizing Its mRNA

(A) The expression of NAE1 increased in the infarction area after MI ($n = 6$). (B) Silencing of RBM15 decreased the expression of NAE1 under hypoxic conditions, ($n = 6$). (C) Overexpression of RBM15 under hypoxic conditions increased the expression of NAE1 mRNA, ($n = 6$). (D) RBM15-RIP qPCR showed that RBM15 was able to bind NAE1 mRNA. (E) qPCR analysis of the expression of NAE1 mRNA after treatment with actinomycin D at the indicated time points from independent experiments. Data are presented as mean \pm SEM. * $P < 0.05$, ** $P < 0.01$, *** $P < 0.001$. In data A, differences were compared with sham. In data B and C, differences were compared with Hypoxia + NC. In data D, difference was compared between IgG and anti-RBM15. In data E, difference was compared between NC and si-RBM15. Data A, B, and C were analyzed using one-way analysis of variance followed by Tukey's post hoc analysis. Data D and E were analyzed using unpaired Student's t test. mRNA = messenger RNA; qPCR = quantitative polymerase chain reaction; other abbreviations as in [Figures 2 and 3](#).

FIGURE 8 Apoptosis of Cardiomyocytes After Inhibition of NAE1



NAE1 showed a protective effect on NRVMs apoptosis under hypoxic conditions. Furthermore, functional evaluations such as NAE1 silencing and using MLN4924 (NAE1 inhibitor) demonstrated that NAE1 played a key role in MI. However, in addition to NAE1, other potential downstream targets of RBM15 might play crucial roles in mediating RBM15 functions in MI protection. Nevertheless, clarifying the exact underlying mechanisms requires further systematic investigations.

Recently, a growing body of work has indicated the essential role of m⁶A in human diseases.⁴⁶⁻⁴⁸ The regulation process involves 3 major m⁶A regulators, including methyltransferase, demethylase, and methylation recognition enzymes. The methyltransferases include METTL3, METTL14, WTAP, RBM15, and RBM15b, but the latter 3 do not have the ability to transfer m⁶A to mRNA. By adding m⁶A to related mRNAs, METTL3 affects the alternative splicing, stable or translation of those mRNA to regulate various diseases.^{43,49-51} During this process, METTL14 mainly binds to some sites in METTL3 to form a new complex, but WTAP and other proteins such as RBM15 or RBM15b probably recruit some factors to assist in the m⁶A regulation process.⁵²⁻⁵⁴ Although some researchers have reported that WTAP and RBM15 can add m⁶A to mRNA to regulate some diseases, they have only found that related phenotypes changed, but they have not investigated whether the exact process of adding m⁶A involves WTAP or RBM15 or not.^{55,56} Therefore, we preferred to name RBM15 as the m⁶A regulator, which can assist the m⁶A adding process.

The present research discussed the regulatory role of RBM15 in the protection from MI and the upregulation of the expression of its targets. It has been reported that RBM15 can facilitate the access of DEP5 to mRNA with its nuclear export factor function.⁵⁷ Yang et al⁵⁸ have demonstrated that Circ-CTNNB1 facilitates RBM15-mediated m⁶A modification to drive aerobic glycolysis and osteosarcoma progression.

Additionally, studies related to RBM15 have focused mainly on its function as an RNA-binding protein, and RBM15 has a great effect on megakaryoblastic leukemia and hematopoietic development.⁵⁹⁻⁶¹ Therefore, in this study, we used RIP assays and multiple loss- or gain-of-function experiments to show that RBM15 can bind NAE1 mRNA and stabilize mRNA to decrease cardiomyocytes apoptosis. NAE1 decreases cell apoptosis mainly through inhibiting the p53 pathway and Akt pathway to regulate the myocardial function in MI.⁶²⁻⁶⁴ Moreover, we found that RBM15 promoted Akt pathway to exert myocardial protective effect (Supplemental Figures 5A and 5B). Finally, these findings envision the RBM15 as a candidate drug for the treatment of MI.

STUDY LIMITATIONS. Although we also found that overexpressing RBM15 could increase the total m⁶A level in cells, and NAE1 was screened from MeRIP-seq, which could be regulated by RBM15, we only drew a conclusion that RBM15 participated in NAE1's m⁶A regulation process because the main methyltransferase was METTL3. Lacking the advanced technologies, we merely showed that RBM15 participated in NAE1's m⁶A regulation process. In terms of the present m⁶A research, how to study the dynamic regulation of m⁶A is extremely important, because the dynamic regulation of methylation and demethylation should be involved in the occurrence and development of diseases. In the future, we will explore more mechanisms of RBM15 in assisting NAE1's m⁶A regulation process. However, our study successfully demonstrated the role of RBM15 in MI protection, suggesting a viable potential for developing targeted therapies against MI.

CONCLUSIONS

The present research shed light on an RNA-binding protein, namely, RBM15, which plays a modulatory function in the regulation of NAE1 mRNA. Regarding

FIGURE 8 Continued

(A) NRVMs were transfected with adenovirus overexpressing NAE1 for 48 hours, and then subjected to hypoxia. The apoptosis markers cleaved-caspase3 and bax, the anti-apoptosis marker bcl-2, and NAE1 protein were assessed by Western blotting; the relative ratios of cleaved-caspase3, bax/bcl-2, NAE1 protein levels were calculated based on the Western blotting result. (n = 6). (B) NRVMs were transfected with si-NAE1 for 48 hours, and then subjected to hypoxia. The apoptosis markers were assessed by Western blotting, and the relative ratios of cleaved-caspase3, bax/bcl2, and NAE1 protein levels were calculated based on the Western blotting results. (n = 6). (C to F) Cell injury was determined by LDH release assay and CCK8 assay. (n = 6). (G) NRVMs were treated with MLN4924 for 24 hours with different concentrations (0.0, 2.5, and 5.0 μM), then the apoptosis markers cleaved-caspase3 and bax, the anti-apoptosis marker bcl-2, and NAE1 protein levels were assessed by Western blotting, and the relative ratios of cleaved-caspase3, bax/bcl2, and NAE1 protein levels were calculated based on Western blotting results. (n = 6). Data are presented as mean ± SEM. *P < 0.05, **P < 0.01, ***P < 0.001. In data A, B, C, D, E, and F, differences were compared with Hypoxia + NC. In data G, difference was compared with Hypoxia + DMSO. All data were analyzed using One-way analysis of variance followed by Tukey's post hoc analysis. si-NAE1 = small interfering NAE1; NRVM = neonatal rat left ventricle myocyte; other abbreviations as in Figures 2 and 7.

the functional implication of NAE1 in MI protection, these findings emphasize the key role of m⁶A in MI. Moreover, the findings of the present research suggest the regulating role of RBM15 as a general mechanism underlying a variety of biological events in MI, which warrants further investigation.

FUNDING SUPPORT AND AUTHOR DISCLOSURES

The work was supported by the Major Research Plan of the National Natural Science Foundation of China (91639104 to Dr Ge), the National Natural Science Fund of China (81521001 to Dr Ge), The Key Research and Development Program sponsored by the Ministry of Science and Technology (2022YFC2407002 to Dr Ma). All other authors have reported that they have no relationships relevant to the contents of this paper to disclose.

ADDRESS FOR CORRESPONDENCE: Dr Jianying Ma, Department of Cardiology, Zhongshan Hospital, Fudan University, 180 Fenglin Road, Shanghai 200032, China. E-mail: ma.jianying@zs-hospital.sh.cn. OR Dr Junbo Ge, Department of Cardiology, Zhongshan Hospital, Fudan University, 180 Fenglin Road, Shanghai 200032, China. E-mail: jbge@zs-hospital.sh.cn.

PERSPECTIVES

COMPETENCY IN MEDICAL KNOWLEDGE: Despite the large number of drug therapies available for the treatment of MI, there remains a compelling need for establishing a novel and effective therapies to improve the efficacy of existing ones. Among many antitumor drugs, the pharmacological basis of many drugs is to promote the apoptosis of tumor cells or inhibit the proliferation of corresponding blood vessels through RNA modification. However, in the cardiovascular field, there is no RNA modification drug for the treatment of MI.

TRANSLATIONAL OUTLOOK: The enhanced m⁶A methylation in the presence of RBM15 overexpression led to the increased expression and stability of NAE1, contributing to less myocardial fibrosis, cell apoptosis, and cardiac dysfunction. Our findings suggest that the enhanced m⁶A level is a protective mechanism in MI, setting the stage for the therapeutic targeting of the MI. Finally, pharmacological inhibitors of the molecules involved the pathway are being tested and are primed for testing for the beneficial effects in patients with MI.

REFERENCES

1. Writing Group M, Mozaffarian D, Benjamin EJ, et al. Heart disease and stroke statistics-2016 update: a report from the American Heart Association. *Circulation*. 2016;133:e38-360.
2. McMurray JJ. Clinical practice. Systolic heart failure. *N Engl J Med*. 2010;362:228-238.
3. Sanders LN, Schoenhard JA, Saleh MA, et al. BMP antagonist gremlin 2 limits inflammation after myocardial infarction. *Circ Res*. 2016;119:434-449.
4. Kiefer JJ, Augoustides JG. Acute myocardial infarction with cardiogenic shock: navigating the invasive options in clinical management. *J Cardiothorac Vasc Anesth*. 2021;35:3154-3157.
5. Chen QQ, Ma G, Liu JF, et al. Neuraminidase 1 is a driver of experimental cardiac hypertrophy. *Eur Heart J*. 2021;42:3770-3782.
6. Madan A, Viswanathan MC, Woulfe KC, et al. TNNT2 mutations in the tropomyosin binding region of TNT1 disrupt its role in contractile inhibition and stimulate cardiac dysfunction. *Proc Natl Acad Sci U S A*. 2020;117:18822-18831.
7. Chen Z, Zhu S, Hong J, et al. Gastric tumour-derived ANGPT2 regulation by DARPP-32 promotes angiogenesis. *Gut*. 2016;65:925-934.
8. Hobohm L, Kolmel S, Niemann C, et al. Role of angiotensin-2 in venous thrombus resolution and chronic thromboembolic disease. *Eur Respir J*. 2021;58.
9. Carpino G, Cardinale V, Di Giamberardino A, et al. Thrombospondin 1 and 2 along with PEDF inhibit angiogenesis and promote lymphangiogenesis in intrahepatic cholangiocarcinoma. *J Hepatol*. 2021;75:1377-1386.
10. Benjamin EJ, Virani SS, Callaway CW, et al. Heart disease and stroke statistics-2018 update: a report from the American Heart Association. *Circulation*. 2018;137:e67-e492.
11. Paik DT, Chandu M, Wu JC. Patient and disease-specific induced pluripotent stem cells for discovery of personalized cardiovascular drugs and therapeutics. *Pharmacol Rev*. 2020;72:320-342.
12. Yamanaka S. Pluripotent stem cell-based cell therapy-promise and challenges. *Cell Stem Cell*. 2020;27:523-531.
13. Wang K, Li Y, Qiang T, Chen J, Wang X. Role of epigenetic regulation in myocardial ischemia/reperfusion injury. *Pharmacol Res*. 2021;170:105743.
14. Lee M, Kim B, Kim VN. Emerging roles of RNA modification: m(6)A and U-tail. *Cell*. 2014;158:980-987.
15. Roundtree IA, Evans ME, Pan T, He C. Dynamic RNA modifications in gene expression regulation. *Cell*. 2017;169:1187-1200.
16. Zaccara S, Jaffrey SR. A unified model for the function of YTHDF proteins in regulating m(6)A-modified mRNA. *Cell*. 2020;181:1582-1595 e18.
17. Zhang B, Wu Q, Li B, Wang D, Wang L, Zhou YL. m(6)A regulator-mediated methylation modification patterns and tumor microenvironment infiltration characterization in gastric cancer. *Mol Cancer*. 2020;19:53.
18. Hu L, Wang J, Huang H, et al. YTHDF1 regulates pulmonary hypertension through translational control of MAGED1. *Am J Respir Crit Care Med*. 2021;203:1158-1172.
19. Mathiyalagan P, Adamiak M, Mayourian J, et al. FTO-dependent N(6)-methyladenosine regulates cardiac function during remodeling and repair. *Circulation*. 2019;139:518-532.
20. Dorn LE, Lasman L, Chen J, et al. The N(6)-methyladenosine mRNA methylase METTL3 controls cardiac homeostasis and hypertrophy. *Circulation*. 2019;139:533-545.
21. Gao XQ, Zhang YH, Liu F, et al. The piRNA CHAPIR regulates cardiac hypertrophy by controlling METTL3-dependent N(6)-methyladenosine methylation of Parp10 mRNA. *Nat Cell Biol*. 2020;22:1319-1331.
22. Wiener D, Schwartz S. The epitranscriptome beyond m(6)A. *Nat Rev Genet*. 2021;22:119-131.
23. Wang X, Wu Y, Guo R, Zhao L, Yan J, Gao C. Comprehensive analysis of N6-methyladenosine RNA methylation regulators in the diagnosis and subtype classification of acute myocardial infarction. *J Immunol Res*. 2022;2022:5173761.
24. Desrosiers R, Friderici K, Rottman F. Identification of methylated nucleosides in messenger RNA from Novikoff hepatoma cells. *Proc Natl Acad Sci U S A*. 1974;71:3971-3975.

25. Zhao BS, Roundtree IA, He C. Post-transcriptional gene regulation by mRNA modifications. *Nat Rev Mol Cell Biol.* 2017;18:31-42.
26. Liu N, Pan T. N6-methyladenosine-encoded epitranscriptomics. *Nat Struct Mol Biol.* 2016;23:98-102.
27. Gong R, Wang X, Li H, et al. Loss of m(6)A methyltransferase METTL3 promotes heart regeneration and repair after myocardial injury. *Pharmacol Res.* 2021;174:105845.
28. Xiao N, Laha S, Das SP, Morlock K, Jesneck JL, Raffel GD. Ott1 (Rbm15) regulates thrombopoietin response in hematopoietic stem cells through alternative splicing of c-Mpl. *Blood.* 2015;125:941-948.
29. Wang T, Kong S, Tao M, Ju S. The potential role of RNA N6-methyladenosine in Cancer progression. *Mol Cancer.* 2020;19:88.
30. Deng X, Su R, Weng H, Huang H, Li Z, Chen J. RNA N(6)-methyladenosine modification in cancers: current status and perspectives. *Cell Res.* 2018;28:507-517.
31. Kechin A, Boyarskikh U, Kel A, Filipenko M. cutPrimers: a new tool for accurate cutting of primers from reads of targeted next generation sequencing. *J Comput Biol.* 2017;24:1138-1143.
32. Kim D, Langmead B, Salzberg SL. HISAT: a fast spliced aligner with low memory requirements. *Nat Methods.* 2015;12:357-360.
33. Meng J, Lu Z, Liu H, et al. A protocol for RNA methylation differential analysis with MeRIP-Seq data and exomePeak R/Bioconductor package. *Methods.* 2014;69:274-281.
34. Yu G, Wang LG, He QY. ChIPseeker: an R/Bioconductor package for ChIP peak annotation, comparison and visualization. *Bioinformatics.* 2015;31:2382-2383.
35. Pertea M, Pertea GM, Antonescu CM, Chang TC, Mendell JT, Salzberg SL. StringTie enables improved reconstruction of a transcriptome from RNA-seq reads. *Nat Biotechnol.* 2015;33:290-295.
36. Robinson MD, McCarthy DJ, Smyth GK. edgeR: a Bioconductor package for differential expression analysis of digital gene expression data. *Bioinformatics.* 2010;26:139-140.
37. Kang PT, Chen CL, Lin P, Zhang L, Zweier JL, Chen YR. Mitochondrial complex I in the post-ischemic heart: reperfusion-mediated oxidative injury and protein cysteine sulfonation. *J Mol Cell Cardiol.* 2018;121:190-204.
38. Wang B, Zhou Q, Bi Y, et al. Phosphatase PPM1L prevents excessive inflammatory responses and cardiac dysfunction after myocardial infarction by inhibiting IKKbeta activation. *J Immunol.* 2019;203:1338-1347.
39. Mehta LS, Beckie TM, DeVon HA, et al. Acute myocardial infarction in women: a scientific statement from the American Heart Association. *Circulation.* 2016;133:916-947.
40. Henry TD, Tomey MI, Tamis-Holland JE, et al. Invasive management of acute myocardial infarction complicated by cardiogenic shock: a scientific statement from the American Heart Association. *Circulation.* 2021;143:e815-e829.
41. Su R, Dong L, Li C, et al. R-2HG exhibits anti-tumor activity by targeting FTO/m(6)A/MYC/CEBPA signaling. *Cell.* 2018;172:90-105 e23.
42. Ries RJ, Zaccara S, Klein P, et al. m(6)A enhances the phase separation potential of mRNA. *Nature.* 2019;571:424-428.
43. Barbieri I, Tzelepis K, Pandolfini L, et al. Promoter-bound METTL3 maintains myeloid leukaemia by m(6)A-dependent translation control. *Nature.* 2017;552:126-131.
44. Shi X, Cao Y, Zhang X, et al. Comprehensive analysis of N6-methyladenosine RNA methylation regulators expression identify distinct molecular subtypes of myocardial infarction. *Front Cell Dev Biol.* 2021;9:756483.
45. Choy M, Xue R, Wu Y, Fan W, Dong Y, Liu C. Role of N6-methyladenosine modification in cardiac remodeling. *Front Cardiovasc Med.* 2022;9:774627.
46. Deng LJ, Deng WQ, Fan SR, et al. m6A modification: recent advances, anticancer targeted drug discovery and beyond. *Mol Cancer.* 2022;21:52.
47. Li Y, Gu J, Xu F, Zhu Q, Chen Y, Ge D, Lu C. Molecular characterization, biological function, tumor microenvironment association and clinical significance of m6A regulators in lung adenocarcinoma. *Brief Bioinform.* 2021;22.
48. Zhang B, Chen Z, Tao B, et al. m(6)A target microRNAs in serum for cancer detection. *Mol Cancer.* 2021;20:170.
49. Vu LP, Pickering BF, Cheng Y, et al. The N(6)-methyladenosine (m(6)A)-forming enzyme METTL3 controls myeloid differentiation of normal hematopoietic and leukemia cells. *Nat Med.* 2017;23:1369-1376.
50. Yankova E, Blackaby W, Albertella M, et al. Small-molecule inhibition of METTL3 as a strategy against myeloid leukaemia. *Nature.* 2021;593:597-601.
51. Liu P, Li F, Lin J, et al. m(6)A-independent genome-wide METTL3 and METTL14 redistribution drives the senescence-associated secretory phenotype. *Nat Cell Biol.* 2021;23:355-365.
52. Chen XY, Zhang J, Zhu JS. The role of m(6)A RNA methylation in human cancer. *Mol Cancer.* 2019;18:103.
53. Zhao Z, Meng J, Su R, Zhang J, Chen J, Ma X, Xia Q. Epitranscriptomics in liver disease: Basic concepts and therapeutic potential. *J Hepatol.* 2020;73:664-679.
54. Jiang X, Liu B, Nie Z, et al. The role of m6A modification in the biological functions and diseases. *Signal Transduct Target Ther.* 2021;6:74.
55. Wang X, Tian L, Li Y, et al. RBM15 facilitates laryngeal squamous cell carcinoma progression by regulating TMBIM6 stability through IGF2BP3 dependent. *J Exp Clin Cancer Res.* 2021;40:80.
56. Li ZX, Zheng ZQ, Yang PY, et al. WTAP-mediated m(6)A modification of lncRNA DIAPH1-AS1 enhances its stability to facilitate nasopharyngeal carcinoma growth and metastasis. *Cell Death Differ.* 2022;29:1137-1151.
57. Zolotukhin AS, Uranishi H, Lindtner S, Bear J, Pavlakis GN, Felber BK. Nuclear export factor RBM15 facilitates the access of DBP5 to mRNA. *Nucleic Acids Res.* 2009;37:7151-7162.
58. Yang F, Liu Y, Xiao J, et al. Circ-CTNBN1 drives aerobic glycolysis and osteosarcoma progression via m6A modification through interacting with RBM15. *Cell Prolif.* 2022:e13344.
59. Kawaguchi H, Hitzler JK, Ma Z, Morris SW. RBM15 and MKL1 mutational screening in megakaryoblastic leukemia cell lines and clinical samples. *Leukemia.* 2005;19:1492-1494.
60. Raffel GD, Mercher T, Shigematsu H, et al. Ott1(Rbm15) has pleiotropic roles in hematopoietic development. *Proc Natl Acad Sci U S A.* 2007;104:6001-6006.
61. Tran NT, Su H, Khodadadi-Jamayran A, et al. The AS-RBM15 lncRNA enhances RBM15 protein translation during megakaryocyte differentiation. *EMBO Rep.* 2016;17:887-900.
62. Ai TJ, Sun JY, Du LJ, et al. Inhibition of neddylation by MLN4924 improves neointimal hyperplasia and promotes apoptosis of vascular smooth muscle cells through p53 and p62. *Cell Death Differ.* 2018;25:319-329.
63. Guihard S, Ramolu L, Macabre C, Wasyluk B, Noel G, Abecassis J, Jung AC. The NEDD8 conjugation pathway regulates p53 transcriptional activity and head and neck cancer cell sensitivity to ionizing radiation. *Int J Oncol.* 2012;41:1531-1540.
64. Ferris J, Espona-Fiedler M, Hamilton C, et al. Pevonedistat (MLN4924): mechanism of cell death induction and therapeutic potential in colorectal cancer. *Cell Death Discov.* 2020;6:61.

KEY WORDS apoptosis, MI therapy, m⁶A, RBM15

APPENDIX For an expanded Methods section as well as supplemental tables and figures, please see the online version of this paper.